

CARBON-EFFICIENCY COUPLED SCHEDULING FOR NEW ENERGY MANUFACTURING SYSTEMS

Pan, H. N. & Wang, M. N.[#]

School of Economics and Management, Inner Mongolia University of Technology, Hohhot 010051, China

E-Mail: wangmengnan@bjtu.edu.cn ([#] Corresponding author)

Abstract

This study addresses the coordination of production efficiency and carbon emissions in new energy manufacturing systems, where fluctuating energy use and carbon intensity complicate scheduling decisions. Conventional simulation-based approaches treat emissions as post-process indicators and fail to capture their interaction with production dynamics. A carbon–efficiency coupled scheduling framework is developed by embedding carbon emissions into the simulation process as dynamic resources. A dual-layer multi-agent structure is constructed, linking load aggregation with manufacturing units. An improved multi-agent reinforcement learning strategy is introduced to coordinate scheduling decisions with real-time carbon signals. A digital twin-based platform is established for validation, and comparative experiments are conducted under multiple scenarios. The results show that carbon emission peaks and total emissions can be reduced while maintaining stable production performance. The proposed framework provides a practical basis for integrating carbon constraints into production scheduling.

(Received in January 2026, accepted in April 2026. This paper was with the authors 5 weeks for 2 revisions.)

Key Words: New Energy Manufacturing Systems, Production Scheduling, Carbon Mitigation Coordination, Production Simulation, Multi-Agent Reinforcement Learning, Digital Twin

1. INTRODUCTION

Under carbon peaking and carbon neutrality targets, new energy manufacturing systems are characterized by concentrated energy consumption and pronounced carbon emission volatility. Coordinating production efficiency with carbon mitigation has therefore become a key challenge for industrial development [1-4]. Production simulation has been widely used for scheduling optimization in discrete manufacturing systems [5, 6]; however, carbon-related objectives are often not explicitly incorporated [7]. As a result, existing approaches are not well suited to dynamic carbon environments or the flexible production requirements of new energy manufacturing systems.

Previous studies have addressed production simulation modelling, multi-objective scheduling, and carbon-oriented scheduling from different perspectives. Simulation research has mainly focused on representing temporal and resource constraints to improve model fidelity [8, 9], while multi-objective scheduling has emphasized production efficiency and cost control through various optimization algorithms [10-13]. Carbon-oriented scheduling has largely relied on process adjustments and energy-efficient equipment to reduce emissions [14-17]. Despite these efforts, important limitations remain when production simulation is combined with carbon–efficiency coordination. Carbon emissions are typically treated as static output indicators [18, 19], rather than decision variables embedded within the simulation process, leading to a separation between carbon accounting and scheduling decisions. In addition, most existing approaches follow a sequential structure in which scheduling is performed before emission evaluation [20], preventing real-time interaction between production flows and carbon flows. Simulation validation is also commonly based on

fixed emission coefficients [21], which cannot reflect fluctuations in grid carbon intensity, thereby limiting practical applicability.

To address these limitations, a carbon–efficiency collaborative scheduling mechanism embedded within a production simulation platform is developed. The approach links carbon quotas with production processes to achieve dynamic coupling between carbon flow and production flow. A dual-layer multi-agent framework is constructed, integrating a game-based interaction mechanism and an improved reinforcement learning strategy to coordinate scheduling decisions with real-time carbon signals. In addition, a simulation-based optimization and validation framework is established to account for dynamic carbon environments and stochastic disturbances.

The remainder of this paper is organized as follows. The problem formulation and simulation scenarios are first presented. The proposed mechanism and its implementation are then described, followed by simulation experiments and result analysis. Finally, conclusions and directions for future work are provided.

2. PROBLEM DESCRIPTION

A new energy manufacturing system is considered, with particular emphasis placed on the full-process production of photovoltaic modules to construct the production simulation scenario. The simulation boundary is defined to encompass core processing operations and key manufacturing units. System operation is required to satisfy multiple constraints, including equipment state transitions, task priority rules, carbon quota limitations, fluctuations in grid carbon intensity, and stochastic disturbances. Among these, the incorporation of novel constraint designs is regarded as a fundamental prerequisite for achieving carbon–efficiency collaborative optimization. A dynamic carbon quota constraint is introduced, in which the workshop-level carbon quota pool is updated in real time based on grid carbon intensity. During process execution, both processing time and carbon quotas are consumed synchronously. When the remaining quota falls below a predefined threshold, a low-carbon operation mode is automatically triggered for the corresponding equipment. The carbon quota update model is formulated as $Q(t) = Q_0 \cdot \eta \cdot \lambda(t)$, where $Q(t)$ denotes the total carbon quota of the workshop at time t ; Q_0 represents the baseline carbon quota, determined by production planning and industry emission standards; η denotes the carbon quota adjustment coefficient, with a value range of $(0, 1]$, which is dynamically adjusted according to the urgency of production tasks; and $\lambda(t)$ denotes the real-time grid carbon intensity at time t , obtained from a regional marginal emission factor database. This formulation extends beyond conventional fixed-quota approaches by enabling dynamic linkage between carbon quotas and grid carbon intensity.

An equipment state–carbon emission coupling constraint is further established, in which equipment operating states – such as processing, standby, start-up/shutdown, and idle – are explicitly associated with dynamic carbon emission factors. The real-time carbon emissions of a single piece of equipment are calculated as $E(t) = P(s(t)) \cdot \lambda(t) \cdot \Delta t$, where $E(t)$ represents the carbon emissions at time t ; $s(t)$ denotes the equipment operating state at time t , taking values from the set {processing, standby, start-up/shutdown, idle}; $P(s(t))$ is the real-time power consumption under state $s(t)$, obtained through empirical data fitting; and Δt is the time interval for emission calculation. This formulation overcomes the limitations of conventional fixed emission coefficients. In addition, an agent interaction constraint is defined to regulate the information exchange mechanisms and decision response latency between the load aggregator agent and manufacturing unit agents. This constraint ensures real-time synchronization between scheduling decisions and simulation execution, thereby accommodating the dynamic nature of production simulation environments.

The core of the carbon–efficiency collaborative scheduling problem lies in achieving multi-objective optimization of production efficiency and carbon mitigation. The optimization objective is formulated as a bi-objective function $\min F = [f_1, f_2]$. The first objective function aims to minimize the makespan, thereby emphasizing production efficiency, and is expressed as:

$$f_1 = \max_{i=1, 2, \dots, n} C_i \quad (1)$$

where, f_1 denotes the makespan; n represents the total number of production tasks; and C_i is the completion time of the i^{th} task, measured in hours. The second objective function aims to minimize total carbon emissions while simultaneously accounting for emission peak control. It is formulated as:

$$f_2 = \sum_{t=1}^T \sum_{j=1}^m E_j(t) \quad (2)$$

where, f_2 denotes the total carbon emissions of the system; T is the total simulation time horizon; m represents the number of manufacturing units; and $E_j(t)$ is the carbon emission of the j^{th} manufacturing unit at time t , calculated according to the previously defined real-time equipment-level emission model. The optimization process is subject to multiple constraints, including equipment flexibility, task due dates, carbon quota limitations, and agent interaction requirements. The resulting scheduling problem is classified as non-deterministic polynomial-time hard. Conventional heuristic algorithms exhibit limited adaptability to real-time scheduling demands under dynamic carbon environments. In addition, static simulation models are unable to capture the coupled effects of grid carbon intensity fluctuations and equipment state transitions, thereby impeding the dynamic balancing of carbon mitigation and production efficiency objectives. Accordingly, the development of advanced optimization algorithms and simulation mechanisms is necessitated to overcome these limitations. This requirement constitutes the fundamental motivation for this study.

3. CORE MECHANISM AND TECHNICAL IMPLEMENTATION

3.1 Carbon–efficiency dual-driven production simulation modelling method

Fig. 1 illustrates the coupling mechanism of the carbon–efficiency dual-driven production simulation. The core innovation of the carbon–efficiency dual-driven modelling approach lies in overcoming the limitation of conventional production simulation, in which carbon emissions are treated as ex-post statistical indicators. Instead, carbon emissions are incorporated as virtual resources embedded within the simulation kernel, enabling deep coupling between production flows and dynamic carbon flows. As a result, both the fidelity and engineering applicability of the simulation model are significantly enhanced, thereby meeting the requirements of dynamic carbon environments in new energy manufacturing systems. The modelling of carbon emission characteristics for manufacturing units is centred on key production equipment. A multi-state carbon emission characteristic library is constructed, in which power transition curves under different operating states are fitted using empirical data. The power fitting model is expressed as $P(s(t)) = a_s \cdot t + b_s$, where $P(s(t))$ denotes the real-time power consumption of equipment under state $s(t)$; $s(t)$ takes values from four operating states: processing, standby, start-up/shutdown, and idle; and a_s and b_s are state-dependent fitting coefficients, calibrated using measured operational data via the least squares method. Based on this power model, dynamic carbon emission factors are further integrated, and carbon emission characteristics are embedded as dynamic attributes within the equipment modules of the simulation platform. This formulation enables real-time linkage between

equipment state transitions and carbon emission variations, thereby ensuring the accuracy of carbon emission calculations during simulation. The modelling of the dynamic carbon quota pool represents a key innovation within the simulation kernel. A virtual workshop-level carbon quota pool is established within the simulation model. Based on real-time carbon intensity signals derived from a regional marginal emission factor database, both the total carbon quota and the unit carbon quota cost are dynamically updated. The carbon quota consumption model is formulated as:

$$Q_{consume}(t) = \sum_{j=1}^m E_j(t) = \sum_{j=1}^m P_j(s_j(t)) \cdot \lambda(t) \cdot \Delta t \quad (3)$$

where, $Q_{consume}(t)$ represents the total carbon quota consumption of the workshop at time t ; m denotes the number of manufacturing units; $P_j(s_j(t))$ is the power consumption of the j^{th} unit under state $s_j(t)$; $\lambda(t)$ denotes the real-time grid carbon intensity at time t ; and Δt is the time interval for calculation. An early-warning mechanism for carbon quotas is further designed. When the remaining carbon quota, $Q_{remain}(t) = Q(t) - Q_{consume}(t)$, falls below a predefined threshold Q_{th} , a low-carbon operation mode is automatically triggered. Carbon quota consumption is reduced by adjusting processing speed and switching to energy-efficient operating conditions. Simultaneously, equipment states are fed back in real time to the scheduling decision module, enabling dynamic interaction between the simulation model and decision-making processes.

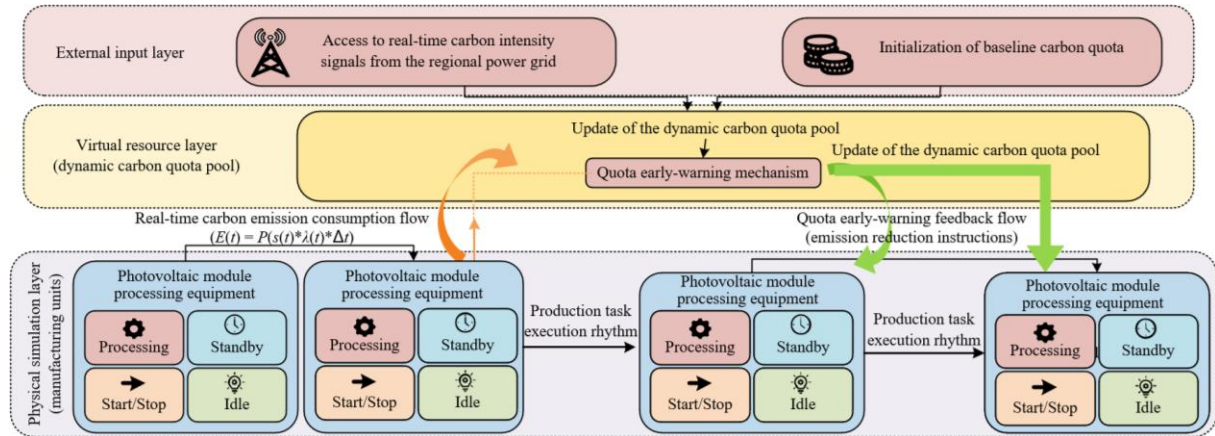


Figure 1: Coupling mechanism of carbon–efficiency dual-driven production simulation.

The coupling logic between carbon flow and production flow constitutes the key mechanism for achieving carbon–efficiency dual-driven simulation modelling. Through a simulation variable association mechanism, variables from three core dimensions – grid carbon intensity fluctuations, equipment carbon emission states, and production task progress – are tightly integrated. Based on this integration, a spatiotemporal evolution model of carbon flow is constructed as follows:

$$E_{total}(x, t) = \sum_{j=1}^m P_j(s_j(x, t)) \cdot \lambda(t) \cdot \Delta t \cdot \omega_j(x) \quad (4)$$

where, $E_{total}(x, t)$ denotes the total carbon flow at spatial location x and time t ; x represents the spatial coordinate of manufacturing units; and $\omega_j(x)$ is the spatial weighting coefficient of the j^{th} equipment, reflecting its relative contribution to the overall carbon flow. By coupling variables across both temporal and spatial dimensions, synchronization between carbon emission calculation and production scheduling is ensured during the simulation process. This formulation effectively resolves the fundamental limitation of conventional production

simulation, in which carbon emission estimation is decoupled from production processes. The modelling framework is fully adapted to the Plant Simulation platform. The carbon emission characteristic library, the dynamic carbon quota pool, and the coupling logic are embedded, respectively, into the equipment modules, the scheduling kernel, and the data interaction modules. Through this modular integration, a simulation model is established. This approach ensures methodological rigor while enhancing scalability and engineering applicability, thereby providing a high-fidelity simulation foundation for subsequent carbon-efficiency collaborative scheduling decisions.

3.2 Multi-agent framework and reinforcement learning optimization

A dual-layer multi-agent framework is established to integrate scheduling decisions with production simulation. The system consists of a load aggregator agent and multiple manufacturing unit agents embedded within the simulation environment. This structure links decision-making with real-time system states and avoids the limitations of centralized scheduling.

The load aggregator operates at the upper layer, coordinating global information, including grid carbon intensity, available carbon quotas, and task queues. Based on these inputs, it issues carbon pricing signals and quota allocation decisions. At the lower layer, each manufacturing unit agent represents a processing unit and makes local decisions according to task urgency and carbon consumption. Information exchange between agents is maintained through a blackboard mechanism, ensuring timely coordination between system-level control and equipment-level actions.

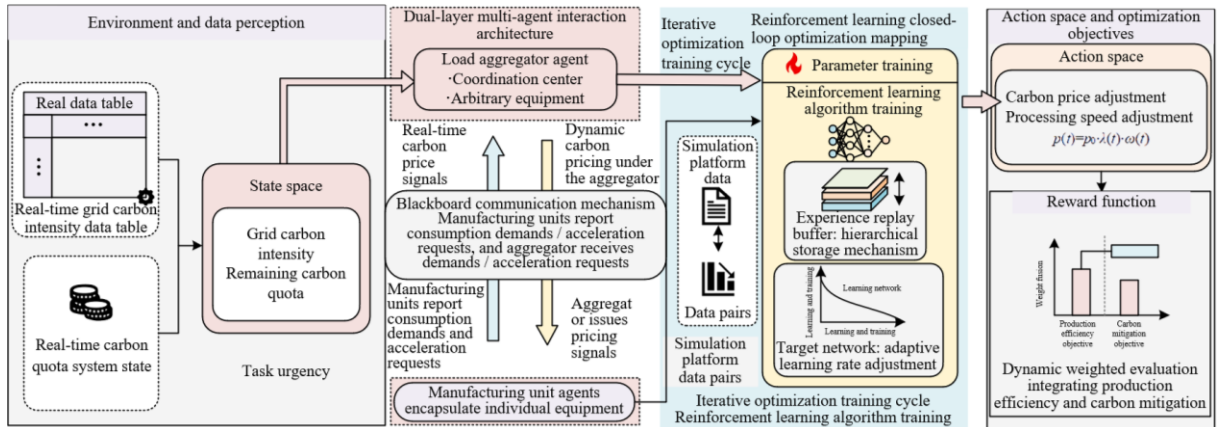


Figure 2: Dual-layer multi-agent collaboration and reinforcement learning optimization framework.

A dynamic game-theoretic mechanism is introduced to enable adaptive optimization of the decision-making process. Manufacturing unit agents submit start-up or acceleration requests based on task urgency and report corresponding carbon quota consumption demands. The load aggregator agent dynamically adjusts carbon prices according to real-time carbon intensity and task urgency weights. The carbon pricing model is defined as $p(t) = p_0 \cdot \lambda(t) \cdot \omega(t)$, where $p(t)$ denotes the real-time carbon price at time t ; p_0 represents the baseline carbon price; $\lambda(t)$ is the real-time grid carbon intensity at time t ; and $\omega(t)$ denotes the task urgency weight, with a value range of $(0, 1]$, where higher carbon intensity or higher task urgency corresponds to higher carbon prices. During simulation execution, this decision logic is directly embedded within the scheduling kernel. Manufacturing unit agents autonomously adjust task execution strategies according to carbon price signals, thereby enabling dynamic balancing between carbon emission peak shaving and production efficiency.

A multi-agent deep reinforcement learning algorithm adapted to production simulation scenarios is developed to address the limitations of conventional algorithms, including low training efficiency and unstable convergence in high-dimensional dynamic environments. An efficient collaborative optimization framework is thereby established. A hierarchical experience replay mechanism is introduced, in which different types of simulation data – such as equipment states, carbon signals, and scheduling decisions – are categorized and stored separately. Storage priorities are assigned based on data importance, thereby improving training efficiency. The target network update strategy is further optimized through the adoption of an adaptive learning rate mechanism. The learning rate adjustment model is defined as $\alpha(t) = \alpha_0 \cdot \exp(-\beta \cdot |F(t) - F^*(t)|)$, where $\alpha(t)$ denotes the adaptive learning rate at time t ; α_0 is the initial learning rate; β represents the decay coefficient; $F(t)$ is the actual value of the carbon–efficiency objective at time t ; and $F^*(t)$ denotes the optimal target value. This formulation effectively mitigates convergence oscillations.

A multi-objective reward function is constructed to integrate production efficiency and carbon mitigation objectives. A dynamic weighting mechanism is introduced to achieve adaptive balancing between the two objectives. The reward function is expressed as $R(t) = \omega_1(t) \cdot R_1(t) + \omega_2(t) \cdot R_2(t)$, where $R(t)$ denotes the total reward at time t ; $\omega_1(t)$ and $\omega_2(t)$ represent the dynamic weights associated with production efficiency and carbon mitigation objectives, respectively, subject to $\omega_1(t) + \omega_2(t) = 1$. When carbon emission peaks exceed predefined thresholds, $\omega_2(t)$ is increased; conversely, when the risk of task delay increases, $\omega_1(t)$ is elevated. The state space encompasses key dynamic variables of the simulation environment, including grid carbon intensity and remaining carbon quota. The action space consists of decision variables such as carbon price adjustment and processing speed regulation, thereby ensuring compatibility with real-time simulation requirements. The training process is tightly integrated with the production simulation platform. Simulation outputs, including makespan and carbon emissions, are utilized as feedback signals for algorithm training. Through iterative simulation–training cycles, the decision policy is progressively optimized. Upon completion of training, the algorithm is embedded into the simulation scheduling module, enabling real-time synchronization between decision-making and simulation execution. This integration ensures both the real-time performance and stability of carbon–efficiency collaborative scheduling.

3.3 Simulation validation under dynamic carbon conditions

A simulation-based validation framework is developed under dynamic carbon conditions, integrating scenario modelling, real-time signal input, and multi-dimensional evaluation. This approach avoids the limitations of static validation settings and allows the proposed mechanism to be assessed under changing carbon environments. A digital twin environment is implemented on the Plant Simulation platform. A representative new energy manufacturing workshop is selected, and the production process is reproduced in detail. Stochastic disturbances, including equipment failures and urgent order arrivals, are incorporated, with parameters calibrated using actual production data. The equipment failure probability model is defined as $P_{fail}(t) = 1 - \exp(-\lambda_{fail} \cdot t)$, where $P_{fail}(t)$ denotes the probability of equipment failure at time t , and λ_{fail} represents the failure rate, determined through fitting of empirical failure data. Urgent order arrivals are modelled as a Poisson process:

$$P(N(t)=k) = \frac{(\lambda_{order}t)^k}{k!} \exp(-\lambda_{order}t) \quad (5)$$

where, $N(t)$ denotes the number of urgent orders at time t , and λ_{order} is the arrival rate of urgent orders. The simulation platform is further integrated with representative daily profiles of regional grid carbon intensity and electricity price, enabling real-time injection of dynamic

carbon signals. The temporal model of carbon intensity is expressed as $\lambda(t) = \lambda_{avg} + A \cdot \sin(2\pi t/T + \varphi) + \varepsilon(t)$, where λ_{avg} denotes the average daily carbon intensity; A is the fluctuation amplitude; T represents the fluctuation period; φ is the initial phase; and $\varepsilon(t)$ is a stochastic disturbance term, introduced to simulate the variability of renewable energy generation and its impact on carbon emissions. Furthermore, the previously proposed carbon–efficiency coupling model and multi-agent reinforcement learning optimization algorithm are embedded. A closed-loop validation framework integrating modelling, decision-making, simulation, and feedback is thereby established. This framework ensures a high degree of consistency between the validation process and real-world production scenarios.

A multi-scenario comparative and multi-dimensional validation design is adopted to highlight the innovation and rigor of the proposed validation framework. Three groups of controlled experiments are designed based on the single-variable principle, namely, a rigid production mode, a static energy-saving mode, and the proposed dynamic collaborative mode. By controlling a single variable in each experiment, the validity of the results is ensured. Three categories of core evaluation metrics are selected to quantify the advantages of the proposed mechanism, including production efficiency, carbon mitigation performance, and system robustness. Among these, robustness is evaluated using the objective deviation rate under stochastic disturbances, defined as:

$$\delta = \frac{|F_{disturb} - F_{normal}|}{F_{normal}} \times 100\% \quad (6)$$

where, δ denotes the objective deviation rate; $F_{disturb}$ represents the objective value under disturbed conditions; and F_{normal} denotes the objective value under normal operating conditions. Visualization outputs from the simulation platform, including Gantt charts, carbon emission fluctuation curves, and Pareto frontiers, are utilized to intuitively demonstrate the effectiveness of the dynamic collaborative mode in achieving carbon emission peak shaving and valley filling, as well as its superiority in carbon–efficiency coordination. Sensitivity analysis is conducted using an orthogonal experimental design. Key influencing parameters, including carbon price fluctuation amplitude, task urgency weight, and equipment flexibility adjustment capability, are selected. Range analysis is performed to determine the relative influence of each parameter on collaborative performance and to identify optimal parameter intervals. Robustness validation is further carried out under extreme scenarios, including abrupt changes in carbon intensity and consecutive equipment failures. The disturbance resistance of the proposed mechanism is evaluated based on objective deviation rates and convergence stability under these extreme conditions. This validation process confirms the applicability of the proposed approach in real-world production environments and further enhances the engineering reliability and scalability of the research outcomes.

4. SIMULATION RESULTS AND ANALYSIS

4.1 Simulation setup

Simulation experiments were carried out on the Plant Simulation 15.0 platform under a Windows 11 environment. The simulation time step was set to 0.1 h, with each run lasting 24 h. Each configuration was repeated ten times, and average results were reported to reduce stochastic effects.

Production data were obtained from a photovoltaic module manufacturing workshop, including equipment parameters, task sequences, and processing times for key operations such as wafer cutting, string soldering, lamination, and framing. The dataset consisted of 20 tasks and 8 processing units. Grid carbon intensity data were sourced from a marginal

emission factor database, with daily values ranging from 0.32 to 0.87 kgCO₂/kWh and an average of 0.58 kgCO₂/kWh.

Model parameters were calibrated using empirical data. Equipment power consumption and emission factors were adjusted to keep deviations within 5% of actual production conditions, ensuring consistency between simulation results and real operations.

4.2 Results analysis

The carbon–efficiency collaborative performance is regarded as the core criterion for evaluating the proposed mechanism. Makespan and equipment utilization were selected as indicators of production efficiency, while total carbon emissions and carbon emission peaks were adopted as indicators of carbon mitigation performance. The comparative results for the three scenarios are presented in Table I.

Table I: Comparison of carbon–efficiency collaborative performance under three scenarios.

Scenario	Scenario 1	Scenario 2	Scenario 3
Scheduling algorithm	Genetic Algorithm	Particle Swarm Optimization	Multi-Agent Deep Reinforcement Learning
Modelling approach	Conventional fixed	Static carbon emission	Carbon–efficiency coupling
Makespan (h)	22.8	23.5	23.9
Equipment utilization (%)	89.6	87.3	88.7
Total carbon emissions (kg CO ₂)	1482.6	1285.3	1212.3
Carbon emission peak (kg CO ₂ /h)	89.7	78.2	68.7
Makespan increase (%)	0.0	3.1	4.8
Total emission reduction (%)	0.0	13.3	18.2
Peak emission reduction (%)	0.0	12.8	23.5

As shown in Table I, the makespan in Scenario 3 increases by only 4.8% compared with Scenario 1. Equipment utilization remains at 88.7%, slightly lower than Scenario 1 but higher than Scenario 2. Total carbon emissions are reduced by 18.2% relative to Scenario 1 and 5.7% relative to Scenario 2, while the emission peak decreases by 23.5% and 12.1%, respectively. These results indicate that emission reduction can be achieved without a noticeable loss in production performance.

Table II: Comparison of algorithm and modelling performance.

Scenario	Scenario 1	Scenario 2	Scenario 3
Scheduling algorithm	Genetic Algorithm	Particle Swarm Optimization	Multi-Agent Deep Reinforcement Learning
Modelling approach	Conventional fixed	Static carbon emission	Carbon–efficiency coupling
Algorithm response time (ms)	386.5	352.8	298.7
Convergence iterations	289	256	198
Modelling fidelity (%)	82.3	85.7	94.6
Response time reduction (%) (vs. Scenario 1)	0.0	8.7	22.7
Iteration reduction (%) (vs. Scenario 1)	0.0	11.4	31.5

Algorithm response time, convergence iterations, and modelling fidelity are further compared in Table II. In Scenario 3, the response time is reduced to 298.7 ms, with decreases of 22.7% and 15.3% compared with Scenarios 1 and 2. The number of iterations drops to 198,

corresponding to reductions of 31.5 % and 22.7 %. Modelling fidelity reaches 94.6 %, improving by 12.3 % and 8.9 %, respectively.

These results show that the proposed approach maintains stable scheduling performance while improving emission outcomes. The integration of carbon-related factors within the simulation also leads to closer agreement with actual production conditions.

4.3 Sensitivity analysis and robustness evaluation

Three parameters – carbon price fluctuation amplitude, task urgency weight, and equipment flexibility – were selected for sensitivity analysis. An orthogonal design with three levels for each parameter was employed, resulting in nine experimental settings. Their effects on carbon-efficiency performance were evaluated, as reported in Table III.

Table III: Sensitivity analysis results of key parameters.

Experiment No.	Carbon price fluctuation amplitude (%)	Task urgency weight	Equipment flexibility adjustment capability (%)	Makespan (h)	Total carbon emissions (kg CO ₂)	Carbon-efficiency composite index
1	10	0.3	50	24.5	1189.6	0.89
2	10	0.5	70	23.7	1208.4	0.92
3	10	0.7	90	23.2	1256.8	0.88
4	20	0.3	70	24.1	1176.3	0.91
5	20	0.5	90	23.5	1197.2	0.94
6	20	0.7	50	23.8	1289.5	0.87
7	30	0.3	90	24.3	1168.5	0.90
8	30	0.5	50	24.0	1243.7	0.86
9	30	0.7	70	23.6	1302.4	0.85

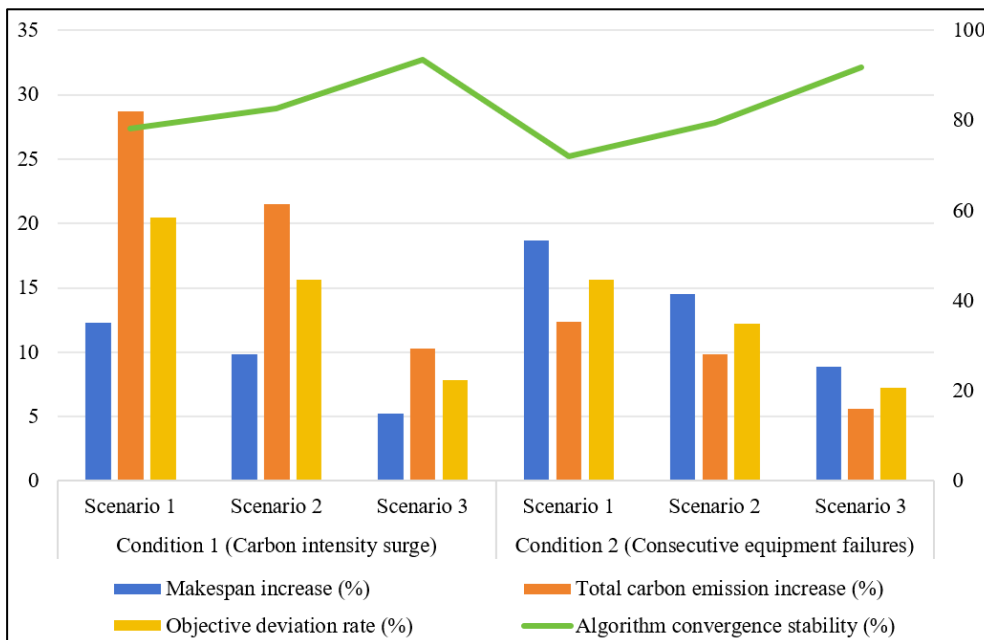


Figure 3: Robustness evaluation results under extreme operating conditions.

Range analysis of Table III shows that task urgency weight has the strongest influence on carbon-efficiency performance, followed by carbon price fluctuation amplitude, while equipment flexibility has a relatively smaller effect. The best performance is obtained when the task urgency weight is 0.5, the carbon price fluctuation amplitude is 20 %, and the

equipment flexibility is 90 %, under which the composite index reaches 0.94. This provides a basis for parameter selection under different production conditions.

Two extreme scenarios were further designed to examine system robustness. In the first case, carbon intensity increases rapidly from 0.58 to 1.02 kg CO₂/kWh within 1 h, reflecting reduced renewable energy supply. In the second case, three key processing units fail continuously for 2 h. The results are shown in Fig. 3. Under both conditions, Scenario 3 exhibits smaller increases in makespan, total emissions, and objective deviation compared with the baseline scenarios. The convergence stability also remains above 90 %, while that of the baseline methods stays below 85 %.

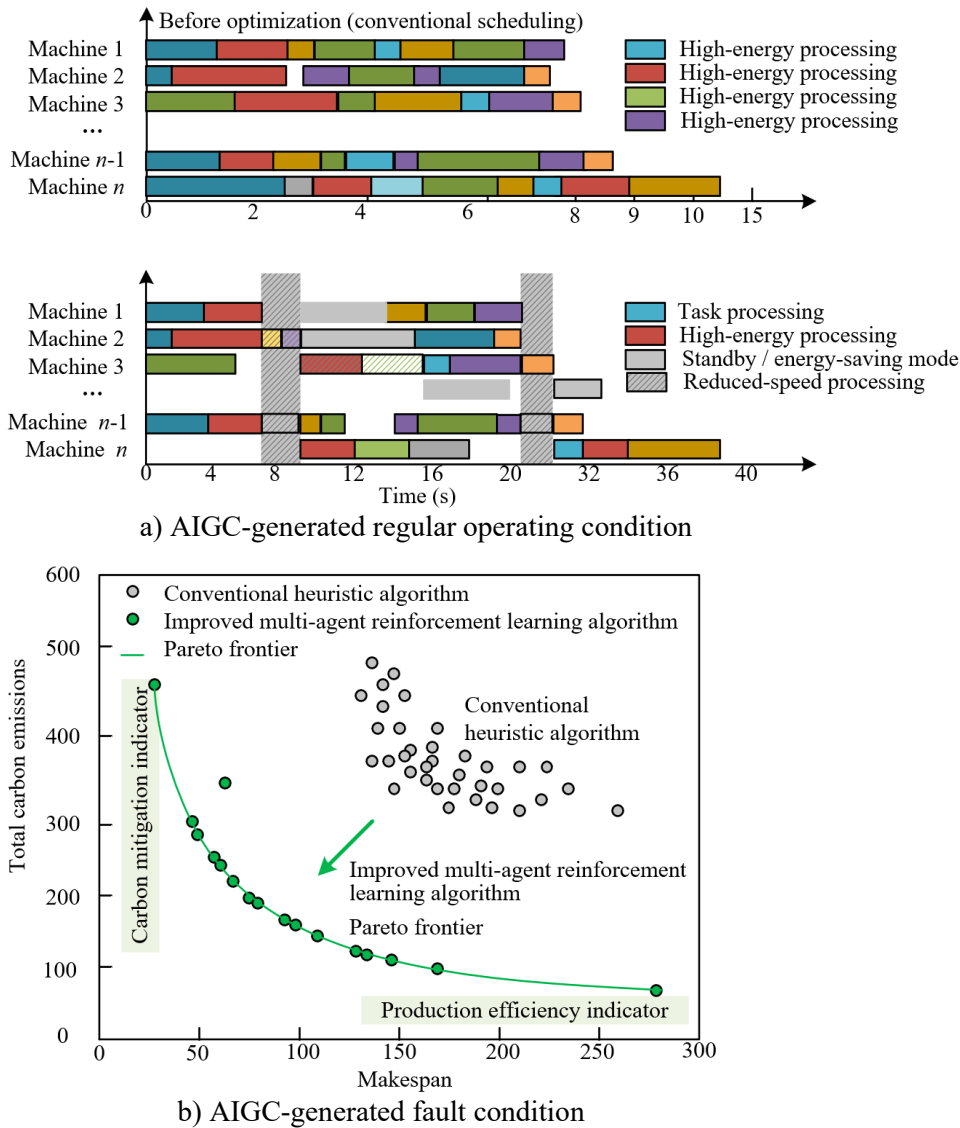


Figure 4: Practical performance of the carbon-efficiency collaborative scheduling mechanism in new energy manufacturing systems.

These results indicate that the proposed mechanism can respond effectively to sudden changes in carbon intensity and equipment failures, maintaining stable performance under disturbed conditions. Comparative experiments were conducted to evaluate scheduling performance before and after carbon-efficiency coordination, as well as bi-objective optimization results. As shown in Fig. 4 a, under conventional scheduling, equipment operates continuously at full load, without considering variations in carbon intensity, leading to concentrated emissions during high-carbon periods. In contrast, the proposed mechanism

identifies high-carbon periods and adjusts operating states, such as standby or speed reduction. Non-urgent tasks are shifted to lower-carbon periods, resulting in better alignment between production load and carbon intensity.

The Pareto frontier in Fig. 4 b further shows that conventional heuristic methods tend to produce solutions in higher-emission regions. The proposed multi-agent reinforcement learning approach yields solutions with lower emissions while maintaining comparable makespan. These results indicate that the proposed method can coordinate production efficiency and carbon emissions more effectively under dynamic conditions.

5. CONCLUSION

To address the critical bottleneck of coordinating production efficiency and carbon mitigation in new energy manufacturing systems under carbon peaking and carbon neutrality targets, as well as the limitations of conventional production simulation in which carbon emissions are decoupled from production processes and scheduling decisions lack dynamic adaptability, a collaborative mechanism for integrating production scheduling and emission reduction was investigated. A carbon–efficiency collaborative optimization framework tailored to production simulation scenarios was proposed and validated. The primary contributions are threefold. First, a carbon–efficiency dual-driven production simulation modelling approach is established, enabling deep coupling between dynamic carbon flow and production flow. Second, a dual-layer multi-agent collaborative framework consisting of load aggregator and manufacturing unit agents is designed. By integrating an improved multi-agent deep reinforcement learning algorithm, dynamic interaction between scheduling decisions and real-time carbon signals is achieved. Third, a high-fidelity simulation validation framework under dynamic carbon environments is constructed, allowing comprehensive and reproducible evaluation of the proposed mechanism.

REFERENCES

- [1] AlGeddawy, T.; ElMaraghy, H. (2016). Design for energy sustainability in manufacturing systems. *CIRP Annals*, Vol. 65, No. 1, 409-412, doi:[10.1016/j.cirp.2016.04.023](https://doi.org/10.1016/j.cirp.2016.04.023)
- [2] Xie, H.; Mohammed, N. (2025). Impact mechanisms of international energy trade on carbon emission intensity under dual-carbon goals, *Journal of Logistics, Informatics and Service Science*, Vol. 12, No. 4, 283-294, doi:[10.33168/JLISS.2025.0415](https://doi.org/10.33168/JLISS.2025.0415)
- [3] Zulkifli Noor, Z. (2025). Sustainable production management in circular economy supply chains, *International Journal of Industrial Engineering and Management*, Vol. 16, No. 2, 204-215, doi:[10.24867/IJIEM-384](https://doi.org/10.24867/IJIEM-384)
- [4] Nasirkhodjaeva, D. S.; Abdullayeva, M. K.; Fayzieva, D. B. (2025). Competitive system as the basis of product quality in Asia: the role of green industry and alternative energy, *International Journal for Quality Research*, Vol. 19, No. 4, 1073-1084, doi:[10.24874/IJQR19.04-01](https://doi.org/10.24874/IJQR19.04-01)
- [5] Liu, A. Y.; Yue, D. Z.; Chen, J. L.; Chen, H. (2024). Deep learning for intelligent production scheduling optimization, *International Journal of Simulation Modelling*, Vol. 23, No. 1, 172-183, doi:[10.2507/IJSIMM23-1-CO4](https://doi.org/10.2507/IJSIMM23-1-CO4)
- [6] He, D. X. (2024). Fault prediction in high-efficiency petroleum machinery production, *International Journal of Simulation Modelling*, Vol. 23, No. 1, 184-195, doi:[10.2507/IJSIMM23-1-CO5](https://doi.org/10.2507/IJSIMM23-1-CO5)
- [7] Cao, K.; Xu, X.; Wu, Q.; Zhang, Q. (2017). Optimal production and carbon emission reduction level under cap-and-trade and low carbon subsidy policies, *Journal of Cleaner Production*, Vol. 167, 505-513, doi:[10.1016/j.jclepro.2017.07.251](https://doi.org/10.1016/j.jclepro.2017.07.251)
- [8] Yang, S. L.; Xu, Z. G.; Wang, J. Y. (2019). Modelling and production configuration optimization for an assembly shop, *International Journal of Simulation Modelling*, Vol. 18, No. 2, 366-377, doi:[10.2507/IJSIMM18\(2\)CO10](https://doi.org/10.2507/IJSIMM18(2)CO10)

- [9] Reggelin, T.; Lang, S.; Schauf, C. (2022). Mesoscopic discrete-rate-based simulation models for production and logistics planning, *Journal of Simulation*, Vol. 16, No. 5, 448-457, doi:[10.1080/17477778.2020.1841575](https://doi.org/10.1080/17477778.2020.1841575)
- [10] Gao, J.; Sun, G.-X.; Qian, T. (2024). Optimization of production scheduling through a multi-objective constrained greedy model, *Journal of Intelligent Management Decision*, Vol. 3, No. 3, 159-174, doi:[10.56578/jimd030303](https://doi.org/10.56578/jimd030303)
- [11] Laili, Y.; Lin, S.; Tang, D. (2020). Multi-phase integrated scheduling of hybrid tasks in cloud manufacturing environment, *Robotics and Computer-Integrated Manufacturing*, Vol. 61, Paper 101850, 18 pages, doi:[10.1016/j.rcim.2019.101850](https://doi.org/10.1016/j.rcim.2019.101850)
- [12] Gao, J.; Yao, M.-T.; Wu, Z.; Deng, X.-Y.; Yu, X.-M.; Yu, L.-N. (2025). Strategic distribution of emergency resources: a multi-objective approach with NSGA-II and prioritization of affected areas, *Journal of Engineering Management and Systems Engineering*, Vol. 4, No. 1, 67-82, doi:[10.56578/jemse040105](https://doi.org/10.56578/jemse040105)
- [13] Madaminov, B.; Saidmurodov, S.; Saitov, E.; Jumanazarov, D.; Alsayah, A. M.; Zhetkenbay, L. (2025). Multi-objective optimization framework for energy efficiency and production scheduling in smart manufacturing using reinforcement learning and digital twin technology integration, *International Journal of Industrial Engineering and Management*, Vol. 16, No. 3, 283-295, doi:[10.24867/IJIEM-389](https://doi.org/10.24867/IJIEM-389)
- [14] Mencaroni, A.; Leyman, P.; Raa, B.; De Vuyst, S.; Claeys, D. (2025). Towards net-zero manufacturing: carbon-aware scheduling for GHG emissions reduction, *Journal of Cleaner Production*, Vol. 529, Paper 146787, 18 pages, doi:[10.1016/j.jclepro.2025.146787](https://doi.org/10.1016/j.jclepro.2025.146787)
- [15] Foumani, M.; Smith-Miles, K. (2019). The impact of various carbon reduction policies on green flowshop scheduling, *Applied Energy*, Vol. 249, 300-315, doi:[10.1016/j.apenergy.2019.04.155](https://doi.org/10.1016/j.apenergy.2019.04.155)
- [16] Jiao, Z. H.; Duan, H. W.; Zhou, Y. J.; Xiang, X. (2025). Low-carbon multimodal vehicle logistics route optimization with timetable limit using Particle Swarm Optimization, Vol. 20, No. 2, 173-190, doi:[10.14743/apem2025.2.534](https://doi.org/10.14743/apem2025.2.534)
- [17] Bhowmik, C.; Zindani, D.; Chatterjee, P.; Marinkovic, D.; Šliogerienė, J. (2025). Evaluation of green energy sources: an extended fuzzy-TODIM approach based on Schweizer-Sklar and power averaging operators, *Facta Universitatis, Series: Mechanical Engineering*, Vol. 23, No. 3, 627-648, doi:[10.22190/FUME240711042B](https://doi.org/10.22190/FUME240711042B)
- [18] Cao, H.; Li, H. (2014). Simulation-based approach to modeling the carbon emissions dynamic characteristics of manufacturing system considering disturbances, *Journal of Cleaner Production*, Vol. 64, 572-580, doi:[10.1016/j.jclepro.2013.10.002](https://doi.org/10.1016/j.jclepro.2013.10.002)
- [19] Mauludin, M. S.; Khairudin, M.; Asnawi, R.; Prasetyo, S. D.; Trisnoaji, Y.; Rizkita, M. A.; Arifin, Z.; Rosli, M. A. M. (2025). Sustainable energy solutions in urban management: carbon emissions and economic assessment of photovoltaic systems at electric vehicle stations in hybrid buildings, *Challenges in Sustainability*, Vol. 13, No. 3, 377-397, doi:[10.56578/cis130305](https://doi.org/10.56578/cis130305)
- [20] Duan, J.; Chen, F.; Feng, M.; Yang, M.; Du, Y. (2026). Sustainable-collaborative scheduling of multi-stage hybrid flowshop with heterogeneous production and transportation using a green scheduling strategy-based NSGA-II-MFO algorithm, *International Transactions in Operational Research*, Vol. 33, No. 3, 1733-1765, doi:[10.1111/itor.13593](https://doi.org/10.1111/itor.13593)
- [21] Nie, L.; Zhang, Q.; Feng, M.; Qin, J. (2024). Research on sustainable collaborative scheduling problem of multi-stage mixed flow shop for crankshaft components, *Scientific Reports*, Vol. 14, Paper 209, 17 pages, doi:[10.1038/s41598-023-49519-x](https://doi.org/10.1038/s41598-023-49519-x)